Nuclear Physics B274 (1986) 1–32
North-Holland, Amsterdam

HELICITY AMPLITUDES FOR HEAVY LEPTON PRODUCTION IN e^+e^- ANNIHILATION

K. HAGIWARA[1,2] and D. ZEPPENFELD[1]

[1] *DESY, Theory Group, Hamburg, F.R. Germany*
[2] *Department of Physics, University of Durham, DH1 3LE, England*

Received 4 December 1985

Signatures of new heavy lepton pair production in e^+e^- annihilation at TRISTAN/SLC/LEP energies are studied in detail. Complete helicity amplitudes for the $2 \to 6$ process $e^+e^- \to L\bar{L} \to (\nu_L f_1 \bar{f}_2)(\bar{\nu}_L f_3 \bar{f}_4)$ are given for arbitrary masses of final fermions and for arbitrary vector and axial vector couplings. Methods to measure the L and ν_L masses, and the neutral- and charged-current couplings of L in terms of four-jet and one-lepton-dijet final state distributions are exemplified. Signatures of heavy neutrino-pair production are discussed briefly. A straightforward method for calculating arbitrary tree amplitudes with external fermions and vector bosons of arbitrary masses is presented for completeness.

1. Introduction

Once the possible observation of the top quark at the CERN collider [1] is confirmed, three families of quarks and leptons are completed, raising as our next immediate question the existence of a fourth generation of fermions. A number of authors have studied the consequences of fourth-generation quarks [2] and leptons [3,4] mainly at hadron colliders, where identification of their signal is the most important task. In e^+e^- annihilation experiments, however, we expect no difficulty in detecting their production simply because the signal cross section constitutes a significant portion of the total annihilation cross section. Here the aim of studies is not the detection of signals but should rather be the determination of detailed properties of the produced particles; their masses, spins and couplings.

In this paper we study in detail the signatures of heavy lepton pair ($L\bar{L}$) production in e^+e^- annihilation at TRISTAN, SCL/LEP-I, and LEP-II energies. The produced heavy leptons are each expected to decay into a neutrino (ν_L) and a fermion-pair ($f\bar{f}'$). The final state will thus contain six partons ($\nu_L\bar{\nu}_L f_1\bar{f}_2 f_3\bar{f}_4$) and typical heavy lepton signals are dilepton (e.g. $e^\pm\mu^\mp$), one-lepton-dijet, and four-jet events with large missing transverse momentum ($\not{p}_T$) due to the escaped neutrinos. All these distributions depend crucially on the mass assumed for the neutrino ν_L and the charged- and neutral-current couplings of the heavy lepton. However,

0550-3213/86/$03.50

because of the missing neutrinos we cannot study the production and decay properties of the heavy leptons separately in actual experiments.

This necessitates theoretical expressions for the exclusive $2 \to 6$ distributions with a certain freedom to change mass and coupling assignments. It is easy to calculate the heavy lepton pair production ($e^+e^- \to L\bar{L}$) cross section even with fixed heavy lepton polarizations. It is also easy to calculate the $L \to \nu_L f_1 \bar{f}_2$ decay distributions for a polarized heavy lepton. However, the final distribution is not simply the product of these cross-sections because the two intermediate heavy lepton polarization states can interfere to give a non-trivial azimuthal angle dependence to the $L \to \nu_L f_1 \bar{f}_2$ decay distribution with respect to the $L\bar{L}$ production plane. This is a novel feature of future heavy lepton searches, where we will be forced to study its properties near the production threshold as compared to the tau-lepton studies [5] where sufficiently high beam energy ($E_b \gtrsim 3m_\tau$) allowed to neglect any such azimuthal angle dependence, even in the correlation studies [6]. Such interference effects between different polarization states of the intermediate heavy lepton can in general lead to non-trivial correlations among final particles near the threshold. Since this inevitably destroys the factorization of the full $2 \to 6$ cross section into the production and the decay parts, we should evaluate directly the $2 \to 6$ process cross section, which requires substantial efforts in the standard method where polarization summed squared matrix elements are evaluated with the help of algebraic manipulation programs, such as REDUCE and SCHOONSCHIP. A full calculation was performed by Kühn and Wagner [7] for the hadronic ($\pi, \rho, A_1, 3\pi$) decay modes of τ leptons. For fourth-generation heavy leptons, we expect jet production to dominate their hadronic decays and the most recent calculation [4] of the squared matrix elements assumes all the six final fermions to be massless and a $V-A$ charged current coupling, and it contains no $\gamma - Z$ interference effects, which is clearly not sufficient for future e^+e^- collider studies.

In this paper we present complete helicity amplitudes for the full $2 \to 6$ process with arbitrary final fermion masses and with arbitrary vector and axial vector couplings of heavy leptons to charged- and neutral-currents. The full amplitude is just a product of the production amplitude and the two decay amplitudes summed over intermediate heavy lepton polarizations. This factorization property of amplitudes allows us to evaluate the basic $2 \to 2$ and $1 \to 3$ amplitudes only, which is straightforward with the method to be described in detail. Final results are very compact and easy to evaluate numerically by computer. We show several distributions for three typical topologies (four-jet plus $\not{p}_T$, one-lepton and a dijet, and dilepton plus $\not{p}_T$ events), in order to examine their sensitivities to the heavy lepton couplings and the heavy neutrino mass.

Direct calculation of helicity amplitudes and their numerical evaluation has a long history [8] but it is only recently that a number of approaches [9–14] appeared as a result of increasing necessity to evaluate complex Feynman amplitudes. A helicity amplitude, being just a complex number, is in principle straightforward to

evaluate for an arbitrary Feynman diagram. Once we choose a particular convention for spinor and vector wave functions, the helicity amplitudes are uniquely determined. A marked property of our approach, which employs the Weyl basis for helicity spinors and the rectangular polarization basis for vector-boson wave functions, is its straightforwardness; no clever choice of bases nor particular techniques for Lorentz contraction of two gamma matrices are required. Because of this straightforwardness, our method leads to an almost unique expression for a given Feynman diagram, which is a useful property when one checks the results obtained by other groups. Final results can be expressed in terms of a simple quantity [12]

$$T(a^\mu, b^\mu)_{\alpha\beta},$$

with $(\alpha, \beta) = (+, +), (+, -), (-, +)$ or $(-, -)$ which gives a complex number as a function of two arbitrary Lorentz four-vectors. This quantity, which was first introduced by Kleiss [12], replaces the role of the Lorentz contraction (the dot-product) of two four-vectors,

$$a \cdot b = a^\mu b_\mu,$$

in terms of which standard squared matrix elements are expressed. Once we set up a routine to evaluate $T(a^\mu, b^\mu)_{\alpha\beta}$, then numerical evaluation of amplitudes is just as straightforward as that of squared matrix elements. We believe that our formalism has some novel features regarding its straightforwardness and we therefore present a complete description of our method to evaluate arbitrary tree amplitudes.

The paper is organized as follows. In sect. 2, we explain the structure of helicity amplitudes for the process $e^+e^- \to L\bar{L} \to (\nu_L f_1 \bar{f}_2)(\bar{\nu}_L f_3 \bar{f}_4)$. In sect. 3, we present our method of evaluating arbitrary tree amplitudes with external fermions and vector bosons. Sect. 4 gives analytic expressions of the production and decay amplitudes with arbitrary external fermion masses and arbitrary vector and axial vector couplings in terms of the quantity $T(a^\mu, {}^\mu)_{\alpha\beta}$. In sect. 5, we present some final state distributions at representative e^+e^- collider energies and examine their sensitivity to the neutrino mass and the heavy lepton couplings. In sect. 6, we briefly discuss the signals of heavy neutral lepton pair production. In sect. 7, we explain how to use our helicity amplitudes to generate distributions for arbitrary transverse or longitudinal polarization of beams. Sect. 8 is reserved for conclusions.

2. Structure of the full helicity amplitudes

Within the standard model, production of a heavy lepton pair $L\bar{L}$ in e^+e^- collisions is mediated by a photon or a Z boson in the s-channel. Subsequently L (and $\bar{L}$) decay into ν_L ($\bar{\nu}_L$) and a virtual W (or a real W if the heavy lepton mass is sufficiently large). The Feynman diagram for the full process is depicted in fig. 1, where the k's, q's, p's and κ's, σ's, λ's denote the four-momenta and helicities of

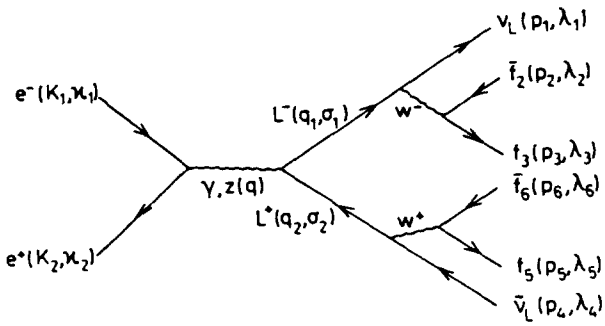

Fig. 1. Feynman graph for production and decay of a heavy lepton pair.

the fermions. For fixed heavy lepton helicities σ_1 and σ_2 the amplitude of the full process can be written as a product of three amplitudes $\mathcal{M}_i$ $(i = 1,2,3)$ where $\mathcal{M}_1$ describes the production of the $L\bar{L}$ pair, while $\mathcal{M}_2$ ($\mathcal{M}_3$) are the decay amplitudes of L ($\bar{L}$). We can hence write the amplitude of the full process as

$$\begin{aligned}\mathcal{M} &= \mathcal{M}(\kappa_1,\kappa_2,\lambda_1,\lambda_2,\lambda_3,\lambda_4,\lambda_5,\lambda_6)\\ &= D_L(q_1^2)D_L(q_2^2)\sum_{\sigma_1=\pm}\sum_{\sigma_2=\pm}\mathcal{M}_1(\kappa_1,\kappa_2,\sigma_1,\sigma_2)\\ &\quad\times\mathcal{M}_2(\sigma_1,\lambda_1,\lambda_2,\lambda_3)\mathcal{M}_3(\sigma_2,\lambda_4,\lambda_5,\lambda_6),\end{aligned} \tag{2.1}$$

where

$$D_X(q^2) = \left[q^2 - m_X^2 + im_X\Gamma_X\right]^{-1} \tag{2.2}$$

denotes the propagator factor of a particle X with mass m_X and width Γ_X.

The amplitudes $\mathcal{M}_i$, $i = 1,2,3$ have identical structure. They are all given by the generic Feynman diagram of fig. 2, where the ψ's stand for either u or v spinors. We use projection operators $P_\pm$ on right- and left-handed spinors

$$P_\pm = \tfrac{1}{2}(1 \pm \gamma_5), \tag{2.3}$$

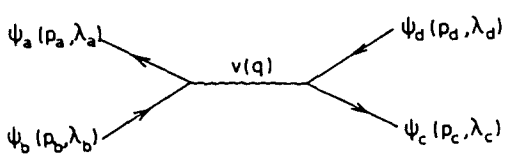

Fig. 2. Generic Feynman graph for vector exchange between fermions.

and right- and left-handed couplings $g_{\pm}^{Vab}$ as defined by the interaction lagrangian

$$\mathcal{L} = e \sum_{\alpha = \pm} g_{\alpha}^{Vab} \bar{\psi}_a \gamma^{\mu} P_{\alpha} \psi_b V_{\mu} . \tag{2.4}$$

with e the magnitude of the electron charge. We can write this generic amplitude as

$$\mathcal{M}_G = -e^2 \sum_{V} D_V^{\mu\nu}(q) \sum_{\alpha = \pm} \sum_{\beta = \pm} g_{\alpha}^{Vab} g_{\beta}^{Vcd} \cdot \bar{\psi}_a \gamma_{\mu} P_{\alpha} \psi_b \cdot \bar{\psi}_c \gamma_{\nu} P_{\beta} \psi_d . \tag{2.5}$$

Here $D_V^{\mu\nu}$ denotes the vector boson propagator. We choose the Feynman gauge for a photon and the unitary gauge for massive vector bosons;

$$D_V^{\mu\nu}(q) = \begin{cases} (-g^{\mu\nu}) D_{\gamma}(q^2) & \text{for } V = \gamma \\ \left(-g^{\mu\nu} + \dfrac{q^{\mu} q^{\nu}}{m_V^2} \right) D_V(q^2) & \text{for } V = W, Z \end{cases} . \tag{2.6}$$

A complete analytic expression for $\mathcal{M}_G$ is given in sect. 4. Each of the amplitudes $\mathcal{M}_i$ $(i = 1, 2, 3)$ are then obtained from it by choosing appropriate couplings. These expressions can easily be evaluated numerically and are then assembled to give the full amplitude via eq. (2.1). The polarization averaged differential cross section is then obtained by

$$d\sigma = \frac{1}{4 k_1 \cdot k_2} \tfrac{1}{2} \cdot \tfrac{1}{2} \sum_{\kappa_1} \sum_{\kappa_2} \left(\prod_{i=1}^{6} \sum_{\lambda_i} \right) |\mathcal{M}|^2 \, d\Phi_6 , \tag{2.7}$$

with the phase space factor

$$d\Phi_6 = (2\pi)^4 \delta^4 \left(k_1 + k_2 - \sum_{i=1}^{6} p_i \right) \prod_{i=1}^{6} \frac{d^3 p_i}{(2\pi)^3 2 E_i} . \tag{2.8}$$

For all heavy lepton masses m_L of interest, the width Γ_L is always much smaller than its mass. We shall hence use the zero width approximation

$$\left| D_L(q^2) \right|^2 = \left| D_{\bar{L}}(q^2) \right|^2 \approx \delta(q^2 - m_L^2) \frac{\pi}{m_L \Gamma_L} \tag{2.9}$$

for calculating cross sections. This together with the trivial overall azimuthal angle integration reduces the original 14-dimensional phase space integration of $d\Phi_6$ to an 11-dimensional one, which considerably facilitates the numerical work.

3. Weyl basis calculation of helicity amplitudes

In this section we present a complete description of our method to evaluate arbitrary tree amplitudes with external fermions and vector bosons. Throughout the paper we employ the Bjorken-Drell notation [15] with only one exception for the normalization of spinors to be explained below.

An arbitrary tree amplitude with external fermions can be expressed in terms of the "fermion string"

$$\bar{\psi}_1 P_\alpha a_1 a_2 \dots a_n \psi_2 , \tag{3.1}$$

where ψ_i denotes a generic four-spinor

$$\psi_i = u(p_i, \lambda_i) \qquad \text{or} \qquad v(p_i, \lambda_i), \tag{3.2}$$

with four-momentum p_i and helicity λ_i,

$$P_\alpha = \tfrac{1}{2}(1 + \alpha\gamma_5), \tag{3.3}$$

with $\alpha = \pm$, and a_i^μ stands for an arbitrary Lorentz four-vector. a_i^μ may be the four-momentum of a particle (p_i^μ), a vector-boson wave function ($\varepsilon^\mu(p_i, \lambda_i)$), an axial vector $\varepsilon^\mu_{\nu\rho\sigma} a_i^\nu a_j^\rho a_l^\sigma$, or another fermion string with uncontracted Lorentz indices,

$$\bar{\psi}_3 P_\beta b_1 b_2 \dots \gamma^\mu \dots b_m \psi_4 . \tag{3.4}$$

For all the spinors and gamma matrices we use the chiral representation where

$$\gamma^\mu = \begin{pmatrix} 0 & \sigma^\mu_+ \\ \sigma^\mu_- & 0 \end{pmatrix}, \tag{3.5}$$

$$\gamma^5 = \begin{pmatrix} -1 & 0 \\ 0 & 1 \end{pmatrix}, \tag{3.6}$$

with the 2×2 matrices

$$\sigma^\mu_\pm = (1, \pm\boldsymbol{\sigma}). \tag{3.7}$$

Here $\boldsymbol{\sigma}$ denotes the Pauli matrices;

$$\boldsymbol{\sigma} = (\sigma^1, \sigma^2, \sigma^3) = \left[\begin{pmatrix} 0 & 1 \\ 1 & 0 \end{pmatrix}, \begin{pmatrix} 0 & -i \\ i & 0 \end{pmatrix}, \begin{pmatrix} 1 & 0 \\ 0 & -1 \end{pmatrix} \right]. \tag{3.8}$$

Next we introduce 2-component Weyl spinors, $(\psi_i)_\pm$, via

$$\psi_i = \begin{pmatrix} (\psi_i)_- \\ (\psi_i)_+ \end{pmatrix}, \qquad \bar{\psi}_i = \left((\psi_i)^\dagger_+, (\psi_i)^\dagger_- \right) \tag{3.9}$$

and the 2×2 matrices $(\not{a})_{\pm}$.

$$\not{a} = a_\mu \gamma^\mu = \begin{pmatrix} 0 & (\not{a})_+ \\ (\not{a})_- & 0 \end{pmatrix}. \tag{3.10}$$

or more explicitly

$$(\not{a})_\pm = a_\mu \sigma^\mu_\pm = \begin{pmatrix} a^0 \mp a^3 & \mp(a^1 - ia^2) \\ \mp(a^1 + ia^2) & a^0 \pm a^3 \end{pmatrix}. \tag{3.11}$$

for arbitrary Lorentz four-vectors a^μ.

By using

$$\bar{\psi}_i P_+ = \left(0, (\psi_i)^\dagger_-\right), \tag{3.12a}$$

$$\bar{\psi}_i P_- = \left((\psi_i)^\dagger_+, 0\right), \tag{3.12b}$$

it is easy to see that the string (3.1) is now replaced by a new string in terms of 2-component spinors and 2×2 matrices:

$$\bar{\psi}_1 P_{-\alpha} \not{a}_1 \not{a}_2 \ldots \not{a}_n \psi_2 = (\psi_1)^\dagger_{\dot{\alpha}} [a_1, a_2, \ldots, a_n]^{\dot{\alpha}} (\psi_2)_{\delta_n \alpha}, \tag{3.13}$$

where

$$[a_1, a_2, \ldots, a_n]^{\dot{\alpha}} = (\not{a}_1)^{\dot{\alpha}} (\not{a}_2)_{-\alpha} \ldots (\not{a}_n)_{\delta_n \alpha}, \tag{3.14}$$

with

$$\delta_n = (-1)^n. \tag{3.15}$$

If one starts with Feynman rules in the 2-component spinor basis, then one directly obtains an expression of the form (3.13).

At this stage, we will in general have contractions of Lorentz indices between different spinor strings (repeated indices within the same string do not appear at the tree level). We get rid of these repeated indices by using the Fierz identities [16],

$$(\sigma^\mu_\pm)_{ij} (\sigma_{\mp\mu})_{kl} = 2\delta_{il}\delta_{kj}, \tag{3.16a}$$

$$(\sigma^\mu_\pm)_{ij} (\sigma_{\pm\mu})_{kl} = 2\left[\delta_{ij}\delta_{kl} - \delta_{il}\delta_{kj}\right], \tag{3.16b}$$

where the spinorial indices i, j, k and l take two values 1 and 2. By denoting a product of the 2×2 matrices of type (3.14) generically by $[s_i]$, an arbitrary

contraction is done by one of the following two rules:

$$(\psi_1)^\dagger_\alpha[s_1]\sigma^\mu_{\mp}[s_2](\psi_2)_\beta\cdot(\psi_3)^\dagger_\gamma[s_3]\sigma_{\mp\mu}[s_4](\psi_4)_\delta$$

$$=2(\psi_1)^\dagger_\alpha[s_1][s_4](\psi_4)_\delta\cdot(\psi_3)^\dagger_\gamma[s_3][s_2](\psi_2)_\beta, \tag{3.17a}$$

$$(\psi_1)^\dagger_\alpha[s_1]\sigma^\mu_{\pm}[s_2](\psi_2)_\beta\cdot(\psi_3)^\dagger_\gamma[s_3]\sigma_{\pm\mu}[s_4](\psi_4)_\delta$$

$$=2(\psi_1)^\dagger_\alpha[s_1][s_2](\psi_2)_\beta\cdot(\psi_3)^\dagger_\gamma[s_3][s_4](\psi_4)_\delta$$

$$-2(\psi_1)^\dagger_\alpha[s_1][s_4](\psi_4)_\delta\cdot(\psi_3)^\dagger_\gamma[s_3][s_2](\psi_2)_\beta. \tag{3.17b}$$

By repeated use of the above contraction formulae, we end up with a product of spinorial strings of the form

$$(\psi_i)^\dagger_\alpha[a_1, a_2, \ldots, a_n]^\alpha(\psi_j)_\beta, \tag{3.18}$$

where none of the four-vectors a^μ_k represents another string. We can hence evaluate the string (3.18) independently.

For this purpose we use helicity eigenstates $\chi_\lambda(p)$

$$\frac{\boldsymbol{\sigma}\cdot\boldsymbol{p}}{|\boldsymbol{p}|}\chi_\lambda(p)=\lambda\chi_\lambda(p) \tag{3.19}$$

as our basis for free spinors*

$$u(p,\lambda)_\alpha=\omega_{+\lambda}(p)\chi_\lambda(p), \tag{3.20a}$$

$$v(p,\lambda)_\alpha=\pm\lambda\omega_{\mp\lambda}(p)\chi_{-\lambda}(p), \tag{3.20b}$$

with

$$\omega_\pm(p)=(E\pm|\boldsymbol{p}|)^{1/2} \tag{3.21}$$

and

$$\chi_+(p)=[2|\boldsymbol{p}|(|\boldsymbol{p}|+p_z)]^{-1/2}\begin{pmatrix}|\boldsymbol{p}|+p_z\\ p_x+ip_y\end{pmatrix}, \tag{3.22a}$$

$$\chi_-(p)=[2|\boldsymbol{p}|(|\boldsymbol{p}|+p_z)]^{-1/2}\begin{pmatrix}-p_x+ip_y\\ |\boldsymbol{p}|+p_z\end{pmatrix}, \tag{3.22b}$$

for an arbitrary momentum $p^\mu=(E,\boldsymbol{p})=(E,p_x,p_y,p_z)$ with $|\boldsymbol{p}|+p_z\neq 0$. When

* Our spinor basis (3.20) satisfies the usual charge conjugation relation [15], $v(p,\lambda)=C\bar{u}^T(p,\lambda)$ with $C=i\gamma^2\gamma^0$. We thank H. Baer and X. Tata for making us aware of the advantage of this convention when dealing with Majorana particles.

$p_z = -|\boldsymbol{p}|$, we choose the convention

$$\chi_+(p) = \begin{pmatrix} 0 \\ 1 \end{pmatrix}. \tag{3.23a}$$

$$\chi_-(p) = \begin{pmatrix} -1 \\ 0 \end{pmatrix}. \tag{3.23b}$$

The free spinors (3.20) satisfy the Dirac equation ($p^2 = m^2$)

$$\not{p}_{\pm} u(p,\lambda)_{\pm} = m u(p,\lambda)_{\mp}, \tag{3.24a}$$

$$\not{p}_{\pm} v(p,\lambda)_{\pm} = -m v(p,\lambda)_{\mp} \tag{3.24b}$$

and are normalised as

$$\bar{u}(p,\lambda) u(p,\lambda) = 2m, \tag{3.25a}$$

$$\bar{v}(p,\lambda) v(p,\lambda) = -2m, \tag{3.25b}$$

which differs from the Bjorken-Drell convention [15]. Because of this normalization, we can use the same phase space factor (see eq. (2.8)) for fermions and bosons.

The formulae (3.20)-(3.23) completely fix our convention for spinors. The most important point is that we express the spinors entirely in terms of their four-momentum in a given frame. Helicities are defined in this particular frame and we should evaluate all the four-momenta in the same frame, a natural choice in e^+e^- collisions being the e^+e^- c.m. frame.

We can now evaluate the spinor-string (3.18) unambiguously in terms of the fermion four-momenta p_i^μ, p_j^μ and the other four-vectors a_k^μ:

$$(\psi_i)_\alpha^\dagger [a_1, \ldots, a_n]^{\alpha}(\psi_j)_\beta$$

$$= C_i C_j \omega_{\alpha\lambda_i}(p_i)\omega_{\beta\lambda_j}(p_j) S(p_i, a_1, \ldots, a_n, p_j)^{\alpha}_{\lambda_i,\lambda_j}, \tag{3.26}$$

where the coefficients C_i and C_j depend on whether the spinors ψ_i and ψ_j correspond to a fermion or an antifermion,

$$C_k = \begin{cases} 1 & \text{for } (\psi_k)_\tau = u(p_k, \lambda_k)_\tau, \\ -\lambda_k \tau & \text{for } (\psi_k)_\tau = v(p_k, -\lambda_k)_\tau. \end{cases} \tag{3.27}$$

These coefficients govern the crossing relations of fermionic amplitudes as exemplified in the next section. The term S on the r.h.s. of eq. (3.26) is uniquely

expressed as

$$S(p_i, a_1, \ldots, a_n, p_j)^{\alpha}_{\lambda_i\lambda_j} = \chi^{\dagger}_{\lambda_i}(p_i)[a_1, \ldots, a_n]^{\alpha}\chi_{\lambda_j}(p_j). \tag{3.28}$$

Our convention is that a subscript λ_i corresponds to the helicity for a fermion, but to the negative of the helicity for an antifermion. This quantity S, which gives a complex number as a function of $(n+2)$ four-momenta and of three two-valued ($+$ or $-$) indices, is the basic quantity in terms of which all the amplitudes should be written. A small algebraic effort to express amplitudes in terms of S as explained in detail in this section not only helps to compare results of different authors but also drastically improves the efficiency of numerical evaluations. A direct numerical evaluation of an amplitude written in four-spinor basis and with Lorentz contractions of different fermion strings is not only technically involved (and may thus easily lead to mistakes) but it is also numerically inefficient.

It is easy to set up a routine to evaluate the complex number S in eq. (3.28). The most straightforward method, which is valid for arbitrary complex four-vectors a^{μ}_k, is to evaluate the 2×2 matrix multiplications recursively by introducing a series of complex two-spinors χ_k $(k = 1, \ldots, n)$:

$$\chi_n = (\not{a}_n)_{\delta_n\alpha}\chi_{\lambda_j}(p_j), \tag{3.29a}$$

$$\chi_k = (\not{a}_k)_{\delta_k\alpha}\chi_{k+1} \qquad \text{for } k = 1, \ldots, n-1, \tag{3.29b}$$

$$S(p_i, a_1, a_2, \ldots, a_n, p_j)^{\alpha}_{\lambda_i\lambda_j} = \chi^{\dagger}_{\lambda_i}(p_i)\chi_1. \tag{3.29c}$$

If all the participating four-vectors are real

$$(a^{\mu}_k)^* = a^{\mu}_k, \tag{3.30}$$

then we can express S entirely in terms of scalar quantities. First we observe the identity

$$(\not{a})_{\mp} = (a)_{\mp}\chi_{\mp}(a)\chi^{\dagger}_{\mp}(a) + (a)_{\pm}\chi_{\pm}(a)\chi^{\dagger}_{\pm}(a), \tag{3.31}$$

with

$$(a)_{\pm} = a^0 \pm |\boldsymbol{a}| \tag{3.32}$$

for an arbitrary real four momentum $a^{\mu} = (a^0, \boldsymbol{a}) = (a^0, a_x, a_y, a_z)$. By replacing all the 2×2 matrices in $[a_1, a_2, \ldots, a_n]^{\alpha}$ via

$$(\not{a}_k)_{\delta_k\alpha} = \sum_{\tau_k = \pm} (a_k)_{\alpha\delta_k\tau_k}\chi_{\tau_k}(a_k)\chi^{\dagger}_{\tau_k}(a_k), \tag{3.33}$$

we obtain the final expression:

$$S(p_i, a_1, a_2, \ldots, a_n, p_j)^{\alpha}_{\lambda_i \lambda_j} = \left[\prod_{k=1}^{n} \sum_{\tau_k = \pm} (a_k)_{\alpha \delta_k \tau_k}\right] T(p_i, a_1)_{\lambda_i \tau_1} T(a_1, a_2)_{\tau_1 \tau_2} \ldots T(a_{n-1}, a_n)_{\tau_{n-1} \tau_n} T(a_n, p_j)_{\tau_n \lambda_j}. \tag{3.34}$$

Here the term T denotes the scalar quantity

$$T(a, b)_{\alpha\beta} = \chi^{\dagger}_{\alpha}(a)\chi_{\beta}(b), \tag{3.35}$$

which can be expressed explicitly as

$$T(a, b)_{++} = N_{ab}^{-1}\left[(|\boldsymbol{a}| + a_z)(|\boldsymbol{b}| + b_z) + (a_x - ia_y)(b_x + ib_y)\right], \tag{3.36a}$$

$$T(a, b)_{+-} = N_{ab}^{-1}\left[-(|\boldsymbol{a}| + a_z)(b_x - ib_y) + (a_x - ia_y)(|\boldsymbol{b}| + b_z)\right], \tag{3.36b}$$

$$T(a, b)_{-+} = -T(a, b)^{*}_{+-}, \tag{3.36c}$$

$$T(a, b)_{--} = T(a, b)^{*}_{++}, \tag{3.36d}$$

with

$$N_{ab} = 2\left[|\boldsymbol{a}|(|\boldsymbol{a}| + a_z)|\boldsymbol{b}|(|\boldsymbol{b}| + b_z)\right]^{1/2}. \tag{3.37}$$

We observe that these are just the spinorial products introduced first by Kleiss [12], which is by no means surprising because our Weyl spinors can be identified with the massless four-spinors used in ref. [12]. These spinorial products satisfy

$$T(a, b)_{\alpha\beta} = T(b, a)^{*}_{\beta\alpha}. \tag{3.38}$$

If one of the three-vectors $\boldsymbol{a}$ or $\boldsymbol{b}$, say $\boldsymbol{a}$, is along the negative z-axis, one needs a special treatment according to our convention (3.23);

$$T(a, b)_{++} = \left[2|\boldsymbol{b}|(|\boldsymbol{b}| + b_z)\right]^{-1/2}(b_x + ib_y), \tag{3.39a}$$

$$T(a, b)_{+-} = \left[2|\boldsymbol{b}|(|\boldsymbol{b}| + b_z)\right]^{-1/2}(|\boldsymbol{b}| + b_z), \tag{3.39b}$$

and the relations (3.36c) and (3.36d) remain valid. The expression (3.34) is particularly useful in two cases. If most of the four-momenta are light-like the conditions

$$(a_k)_{-} = 0 \qquad \text{if } a_k^0 = |\boldsymbol{a}_k| \tag{3.40}$$

get rid of most of the summations over τ_k's, and if the number of 2×2 matrices (n) is small, very simple expressions arise. For $n \leqslant 2$ we obtain

$$S(p,k)^{a}_{\lambda\sigma} = T(p,k)_{\lambda\sigma}, \tag{3.41a}$$

$$S(p,a,k)^{a}_{\lambda\sigma} = \sum_{\tau=\pm} (a)_{-a\tau} T(p,a)_{\lambda\tau} T(a,k)_{\tau\sigma}, \tag{3.41b}$$

$$S(p,a,b,k)^{a}_{\lambda\sigma} = \sum_{\tau=\pm} \sum_{\rho=\pm} (a)_{-a\tau} (b)_{a\rho} T(p,a)_{\lambda\tau} T(a,b)_{\tau\rho} T(b,k)_{\rho\sigma}. \tag{3.41c}$$

In our particular example of heavy lepton pair production and their decays, we encounter $n = 0$ and $n = 1$ cases only and all the final results are expressed directly in terms of the quantity T instead of S.

For completeness we add two general comments regarding our formalism even though we do not need them for the problem at hand.

(i) Strictly speaking, we should assign a number (real or complex) to the quantity $\omega_\pm(p)$ appearing in eq. (3.26) only for the on-shell momentum

$$p^0 = E = \left[|\boldsymbol{p}|^2 + m^2\right]^{1/2}. \tag{3.42}$$

As exemplified in the previous section, it is still possible to combine two amplitudes with a common fermion leg via

$$\sum_{\lambda} \mathcal{M}_1[(p,\lambda),\ldots]\,\mathcal{M}_2[(p,\lambda),\ldots]\,D(p^2), \tag{3.43}$$

interpreting the fermion now as an intermediate state. Once this intermediate state gets virtual, however, the $\omega_\pm(p)$ can no longer be well defined, because their products must satisfy the following conditions,

$$\omega_+(p)\omega_-(p) = m, \tag{3.44a}$$

$$\omega_\pm(p)\omega_\mp(p) = p^0 \pm |\boldsymbol{p}| = (p)_\pm. \tag{3.44b}$$

This convention is needed in order to obtain the correct propagator factors in 4×4 notation:

$$\begin{aligned}
&\sum_{\lambda} u(p,\lambda)\bar{u}(p,\lambda) \\
&\quad = \sum_{\lambda} \begin{pmatrix} \omega_{-\lambda}(p)\omega_\lambda(p)\chi_\lambda(p)\chi_\lambda^\dagger(p) & \omega_{-\lambda}(p)\omega_{-\lambda}(p)\chi_\lambda(p)\chi_\lambda^\dagger(p) \\ \omega_\lambda(p)\omega_\lambda(p)\chi_\lambda(p)\chi_\lambda^\dagger(p) & \omega_\lambda(p)\omega_{-\lambda}(p)\chi_\lambda(p)\chi_\lambda^\dagger(p) \end{pmatrix} \\
&\quad = \begin{pmatrix} m & \not{p}_- \\ \not{p}_+ & m \end{pmatrix} = \not{p} + m
\end{aligned} \tag{3.45}$$

and similarly for antifermions. When dealing with virtual intermediate fermions, only the product $\mathcal{M}_1\mathcal{M}_2$ is defined in eq. (3.43), which is expressed in terms of S's and the assignment (3.44). This point is important when finite width effects have to be considered. Since we are working in the zero width approximation, we need not worry about this point.

(ii) In order to take advantage of the simple formulae (3.41) and (3.34), all the four-vectors, in particular all the vector-boson polarization vectors should be real. This prevents us from using the helicity basis for vector bosons unless we express the polarization vectors entirely in terms of other momenta (as in the CALKUL basis [11]) which is just an unnecessary complexity in our formalism. We thus choose a rectangular basis [9] for our standard vector-boson wave functions. Just as the spinors in eq. (3.22), the polarization vectors are expressed entirely in terms of vector-boson four-momenta,

$$k^\mu = (E, k_x, k_y, k_z). \tag{3.46a}$$

$$E = \left[|\boldsymbol{k}|^2 + m^2\right]^{1/2}. \tag{3.46b}$$

$$k_T = \left[(k_x)^2 + (k_y)^2\right]^{1/2}. \tag{3.46c}$$

as follows:

$$\varepsilon^\mu(k, \lambda = 1) = (|\boldsymbol{k}| k_T)^{-1}\left(0, k_x k_z, k_y k_z, -k_T^2\right), \tag{3.47a}$$

$$\varepsilon^\mu(k, \lambda = 2) = (k_T)^{-1}(0, -k_y, k_x, 0), \tag{3.47b}$$

$$\varepsilon^\mu(k, \lambda = 3) = (E/m|\boldsymbol{k}|)\left(|\boldsymbol{k}|^2/E, k_x, k_y, k_z\right). \tag{3.47c}$$

It is easy to verify the following identities, satisfied by the above polarization vectors,

$$k_\mu \varepsilon^\mu(k, \lambda) = 0. \tag{3.48a}$$

$$\varepsilon_\mu(k, \lambda)\varepsilon^\mu(k, \lambda') = -\delta_{\lambda\lambda'}. \tag{3.48b}$$

Massless vector bosons have only two polarization states, $\lambda = 1$ and 2, on their mass-shell. Helicity eigenvectors are expressed as

$$\varepsilon^\mu(k, \lambda = \pm) = \sqrt{\tfrac{1}{2}}\left[\mp\varepsilon^\mu(k, \lambda = 1) - i\varepsilon^\mu(k, \lambda = 2)\right]. \tag{3.49}$$

Hence whenever one needs helicity amplitudes, they are obtained from our standard

amplitudes via

$$\mathcal{M}(\{k,\lambda=\pm\},\ldots)=\sqrt{\tfrac{1}{2}}\left[\mp\mathcal{M}(\{k,\lambda=1\},\ldots)-i\mathcal{M}(\{k,\lambda=2\},\ldots)\right]. \quad (3.50)$$

4. Analytic form of production and decay amplitudes

We are now in a position to express the amplitudes $\mathcal{M}_i$, $i=1,2,3$ of eq. (2.1) in terms of the quantities ω and T introduced in the last section. In order to be able to treat t- and b-quarks in the final state as well as a non-negligible mass of ν_L, we allow all the fermion masses to be arbitrary.

By contracting the vector boson propagator factors, and by using the Fierz identities, eq. (3.16), the generic amplitude (2.5) can be cast into the form

$$\begin{aligned}\mathcal{M}_{C_i}=2e^2\sum_V D_V(q^2)\sum_{\alpha=\pm}\sum_{\beta=\pm} g_\alpha^{Vab}g_\beta^{Vcd}\\ \times\Big\{\delta_{\alpha\beta}\big[(\psi_a)_\alpha^\dagger(\psi_b)_\alpha\cdot(\psi_c)_\beta^\dagger(\psi_d)_\beta-(\psi_a)_\alpha^\dagger(\psi_d)_\beta\cdot(\psi_c)_\beta^\dagger(\psi_b)_\alpha\big]\\ +\delta_{\alpha,-\beta}(\psi_a)_\alpha^\dagger(\psi_d)_\beta\cdot(\psi_c)_\beta^\dagger(\psi_b)_\alpha\\ -\tfrac{1}{2}\varepsilon_V(\psi_a)_\alpha^\dagger(q)_\alpha(\psi_b)_\alpha\cdot(\psi_c)_\beta^\dagger(q)_\beta(\psi_d)_\beta\Big\}, \quad (4.1a)\end{aligned}$$

with

$$\varepsilon_V=\begin{cases}0 & \text{for } V=\gamma,\\ 1/m_V^2 & \text{for } V=W,Z.\end{cases} \quad (4.1b)$$

The term proportional to ε_V survives only when the massive vector boson couples exclusively to non-conserved currents and is non-negligible only for the $L\to\nu_L\bar{b}$ decay in the present example. With the help of eqs. (3.26) and (3.41), we obtain the standard form of the generic amplitude

$$\begin{aligned}\mathcal{M}_{C_i}=2e^2\sum_V D_V(q^2)\sum_{\alpha=\pm}\sum_{\beta=\pm} g_\alpha^{Vab}g_\beta^{Vcd}\omega_{a\lambda_a}(p_a)\omega_{b\lambda_b}(p_b)\omega_{c\lambda_c}(p_c)\omega_{d\lambda_d}(p_d)\\ \times C_{C_i}\Big\{\delta_{\alpha\beta}T(p_a,p_b)_{\lambda_a\lambda_b}T(p_c,p_d)_{\lambda_c\lambda_d}\\ +(\delta_{\alpha,-\beta}-\delta_{\alpha\beta})T(p_a,p_d)_{\lambda_a\lambda_d}T(p_c,p_b)_{\lambda_c\lambda_b}\\ -\tfrac{1}{2}\varepsilon_V S(p_a,q,p_b)^\alpha_{\lambda_a\lambda_b}S(p_c,q,p_d)^\beta_{\lambda_c\lambda_d}\Big\}, \quad (4.2)\end{aligned}$$

where the factor $C_{C_i}=C_aC_bC_cC_d$ is determined by the crossing property of each

process via eq. (3.27) and turns out to be

$$C_G = \begin{cases} \alpha\beta k_2\sigma_2 & \text{in } \mathcal{M}_1 \\ -\beta\lambda_2 & \text{in } \mathcal{M}_2 \\ -\beta\sigma_2\lambda_4\lambda_6 & \text{in } \mathcal{M}_3 \end{cases} \tag{4.3}$$

This general expression suffices for determining all three amplitudes. The relevant momenta, helicities, and the standard model couplings to insert for each process can be inferred from table 1. One merely has to observe that for antiparticles helicities are reversed in the generic amplitude (4.2) (see eq. (3.20) and table 1).

In the following we show more explicit formulae for the process by choosing the standard model couplings (table 1), neglecting the electron mass, and by using the physical helicities for antiparticles to demonstrate our notation clearly. More general cases can easily be inferred from the generic formula (4.2).

In the heavy lepton decay $L \to \nu_L \bar{f}_2 f_3 (\mathcal{M}_2)$, only the W boson is exchanged with left-handed couplings ($\alpha = \beta = -$) to fermions. Furthermore, we can simplify the last term in the generic expression (4.1) by making use of the Dirac equations (3.24). The result of the substitution reads

$$\begin{aligned}
&\mathcal{M}_2(q_1, \sigma_1; p_i, \sigma_i; i = 1,2,3) \\
&\quad = 8\pi\alpha D_W\big((p_2+p_3)^2\big) g_-^{W\nu_l L} g^{Wf_2f_3}\lambda_2 \\
&\qquad \times \Big\{ \omega_{-\sigma_1}(q_1)\omega_{-\lambda_1}(p_1)\omega_{\lambda_2}(p_2)\omega_{\lambda_1}(p_3) \\
&\qquad\quad \times \big[T(p_1,q_1)_{\lambda_1,\sigma_1} T(p_3,p_2)_{\lambda_1,-\lambda_2} - T(p_1,p_2)_{\lambda_1,-\lambda_2} T(p_3,q_1)_{\lambda_1,\sigma_1}\big] \\
&\qquad\quad - \frac{1}{2m_W^2}\big[m_L\omega_{-\lambda_1}(p_1)\omega_{\sigma_1}(q_1) - m_1\omega_{\lambda_1}(p_1)\omega_{-\sigma_1}(q_1)\big] \\
&\qquad\quad \times \big[m_2\omega_{-\lambda_2}(p_2)\omega_{-\lambda_1}(p_3) + m_3\omega_{\lambda_2}(p_2)\omega_{\lambda_1}(p_3)\big] \\
&\qquad\quad \times T(p_1,q_1)_{\lambda_1,\sigma_1} T(p_3,p_2)_{\lambda_1,-\lambda_2} \Big\},
\end{aligned} \tag{4.4}$$

where $\alpha = e^2/4\pi$, $m_1 = m_{\nu_L}$, $m_2 = m_{f_2}$, $m_3 = m_{f_3}$. In most cases of interest this amplitude can be simplified significantly. First, the expression (4.4) makes it explicit that the latter term proportional to $1/m_W^2$ is important only when m_2/m_W or m_3/m_W is non-negligible, i.e., for the $L \to \nu_L \bar{t}b$ decay only (if fourth-generation quarks are heavier than L). Second, the relation

$$\lim_{p^2 \to 0} \omega_\lambda(p) = \delta_{\lambda,+}\sqrt{2p^0} \tag{4.5}$$

TABLE 1
Coupling constants and spinors to be inserted in the generic amplitude (4.1) in case of $L\bar{L}$ production ($\mathcal{M}_1$), L decay ($\mathcal{M}_2$), and $\bar{L}$ decay($\mathcal{M}_3$)

Generic case	$\mathcal{M}_1$	$\mathcal{M}_2$	$\mathcal{M}_3$
$\psi_a(p_a, \lambda_a)$	$v(k_2, -\kappa_2)$	$u(p_1, \lambda_1)$	$v(q_2, -\sigma_2)$
$\psi_b(p_b, \lambda_b)$	$u(k_1, \kappa_1)$	$u(q_1, \sigma_1)$	$v(p_4, -\lambda_4)$
$\psi_c(p_c, \lambda_c)$	$u(q_1, \sigma_1)$	$u(p_3, \lambda_3)$	$u(p_5, \lambda_5)$
$\psi_d(p_d, \lambda_d)$	$v(q_2, -\sigma_2)$	$v(p_2, -\lambda_2)$	$v(p_6, -\lambda_6)$
$g_+^{Vab} = g_+^{Vcd}$	$\begin{cases} -1 & \gamma \\ \tan\theta_W & Z \end{cases}$	0	0
$g_-^{Vab} = g_-^{Vcd}$	$\begin{cases} -1 & \gamma \\ \dfrac{-\frac{1}{2} + \sin^2\theta_W}{\sin\theta_W \cos\theta_W} & Z \end{cases}$	$\dfrac{1}{\sqrt{2}\sin\theta_W}$	$\dfrac{1}{\sqrt{2}\sin\theta_W}$

reduces the number of non-vanishing amplitudes whenever a light fermion exists. Hence if the condition

$$m_{f_2}^2, m_{f_1}^2 \ll m_L^2 \tag{4.6}$$

is satisfied, the formula (4.4) reduces to

$$\mathcal{M}_2 = \frac{4\pi\alpha}{\sin^2\theta_W} D_W\big((p_2+p_3)^2\big) 2\sqrt{p_2^0 p_3^0}\, \delta_{\lambda_2,\ \ } \delta_{\lambda_1,\ \ } \omega_{\ \ \sigma_1}(q_1)\omega_{\ \ \lambda_1}(p_1)$$
$$\times \big[T(p_1, q_1)_{\lambda_1,\sigma_1} T(p_3, p_2)_{\ \ \ \ } - T(p_1, p_2)_{\lambda_1,\ \ } T(p_3, q_1)_{\ \ \sigma_1}\big], \tag{4.7}$$

which still incorporates exact m_{ν_1} dependence.

The amplitude for $\bar{L}$ decay is related to eq. (4.4) by the crossing relations given in table 1 and by the property (3.38) of the T's: Up to the overall phase factor given in eq. (4.3) it is obtained from eq. (4.4) by the substitution

$$(q_1, \sigma_1;\ p_1, \lambda_1;\ p_2, \lambda_2;\ p_3, \lambda_3) \to (q_2, -\sigma_2;\ p_4, -\lambda_4;\ p_5, -\lambda_5;\ p_6, -\lambda_6) \tag{4.8}$$

and by taking the complex conjugate of the full amplitude except the propagator factor D_W. In the simplified case where f_5 and f_6 masses are negligible, we find explicitly

$$\mathcal{M}_3 = \frac{4\pi\alpha}{\sin^2\theta_W} D_W\big((p_5+p_6)^2\big) 2\sqrt{p_5^0 p_6^0}\, \delta_{\lambda_5,\ \ -}\delta_{\lambda_6,\ \ +}\omega_{\sigma_2}(q_2)\omega_{\lambda_4}(p_4)\sigma_2\lambda_4$$
$$\times \big[T(q_2, p_4)_{\ \ \sigma_2,\ -\lambda_4} T(p_5, p_6)_{\ \ \ \ \ \ } - T(p_5, p_4)_{\ \ \ \lambda_4} T(q_2, p_6)_{\ \ \sigma_2,\ \ }\big]. \tag{4.9}$$

Neglecting light fermion masses is even more justified for the production amplitude ($\mathcal{M}_1$) for $e^+e^- \to L\bar{L}$. In the $m_e = 0$ limit it is given by

$$\begin{aligned}\mathcal{M}(e^+e^- \to L\bar{L}) &= \mathcal{M}_1(k_i, \kappa_i; q_i, \sigma_i;\ i = 1,2) \\ &= -8\pi\alpha 2\sqrt{k_1^0 k_2^0}\,\delta_{\kappa_1,-\kappa_2}\kappa_2\sigma_2 \sum_{V=\gamma,Z} D_V(s) g_{\kappa_1}^{Vee} \\ &\quad \times \Big\{ \Big[g_{\kappa_1}^{VLL}\omega_{\kappa_1\sigma_1}(q_1)\omega_{\kappa_2\sigma_2}(q_2) + g_{-\kappa_1}^{VLL}\omega_{\kappa_2\sigma_1}(q_1)\omega_{\kappa_1\sigma_2}(q_2) \Big] \\ &\qquad \times T(k_2, q_2)_{-\kappa_2,-\sigma_2} T(q_1, k_1)_{\sigma_1,\kappa_1} - g_{\kappa_1}^{VLL}\omega_{\kappa_1\sigma_1}(q_1)\omega_{\kappa_2\sigma_2}(q_2) \\ &\qquad \times T(k_2, k_1)_{-\kappa_2,\kappa_1} T(q_1, q_2)_{\sigma_1,-\sigma_2} \Big\}. \end{aligned} \tag{4.10}$$

When working in the e^+e^- c.m. frame the last term in eq. (4.10) vanishes identically. This happens because

$$T(k_2, k_1)_{-\kappa_2,\kappa_1}\big|_{\kappa_2=-\kappa_1} = \chi^\dagger_{\kappa_1}(-k_1)\chi_{\kappa_1}(k_1) = 0 \tag{4.11}$$

by virtue of the orthogonality properties of helicity eigenstates. It should be noticed, however, that dropping this term spoils the Lorentz-covariance of the amplitude.

In the calculations performed for producing the graphs of the next section we have made use of the zero mass approximation for the decay products of virtual (or real) W's. It is amusing, however, that the complete expressions, including all mass effects, can be written down so simply.

5. Heavy lepton signals

The expressions derived for the amplitudes in the previous section can easily be evaluated numerically and assembled to give the complete differential cross section $d\sigma/d\Phi_6$. We have written a Fortran program for this purpose, which then uses the Monte Carlo integration routine VEGAS [17] in order to perform the 11-dimensional phase space integral.

The program was checked as follows. First the Lorentz invariance of $d\sigma/d\Phi_6$ was verified numerically. Second, it reproduces some well known quantities, the total cross section, the heavy lepton decay width and the heavy lepton polar angle distribution. Further qualitative tests were made by reproducing the distribution given by Baer et al. [4]. Numerical efficiency of the algorithm is found satisfactory; on an IBM 3081 various distributions are generated with 10^5 phase space points in 6 CPU minutes of which more than $\frac{1}{3}$ is used to set up phase space and fill numbers of histograms.

Heavy leptons, once they are produced, will either decay leptonically into $\nu\bar{\nu}e$, $\nu\bar{\nu}\mu$, $\nu\bar{\nu}\tau$ or hadronically into $\nu\bar{u}d$, $\nu\bar{c}s$ with ratios 1 : 1 : 1 : 3 : 3. Decays into $\nu\bar{t}b$ are negligible at TRISTAN or LEP/SLC energies: a 45 GeV heavy lepton has a branching fraction into $\nu\bar{t}b$ well below 1% even if optimistic values like $m_t = 30$ GeV, $m_{\nu_L} = 0$ are assumed. This is not true any more for LEP II energies: the decay products of a heavy lepton pair with $m_L = 90$ GeV may contain a top quark with more than 30% probability if the top mass is low enough. In the following we will not consider the $\nu\bar{t}b$ decay mode of heavy leptons and hence some exercise on its effects should be made at LEP II energies before a more realistic confrontation is made. Likewise, we do not study the effects caused by τ decays. Its leptonic decay contaminates the e + dijet and μ + dijet signal in the low lepton energy tail. Cuts in final lepton energy can easily make the τ contribution negligible. Its hadronic decay produces a single very narrow jet as opposed to dijets from direct heavy lepton decay and should easily be distinguished. Anyway, it is a straightforward exercise [18] to implement polarized τ decay distributions in our algorithm.

The observed signals of $L\bar{L}$ production can be classified according to their jet content:

(a) $L\bar{L} \to \nu_L\bar{\nu}_\ell q_1\bar{q}_2q_3\bar{q}_4$ resulting in 4 jets + missing momentum.

(b) $L\bar{L} \to \ell^+ q_1\bar{q}_2 + 3$ neutrinos resulting in a dijet + charged lepton + missing momentum signal.

(c) $L\bar{L} \to \ell^+\ell'^-$ + neutrinos producing an opposite sign dilepton + missing momentum signal.

The probabilities of the three classes are roughly 44 : 35 : 7 when τ leptonic decays are included. The common feature of all the $L\bar{L}$ decay modes is missing four-momentum carried away by the neutrinos. This together with the charged leptons or

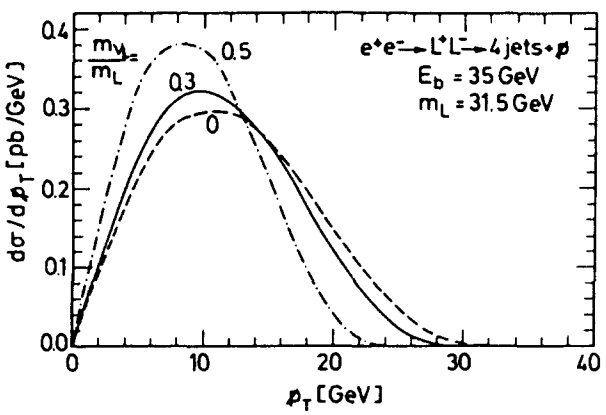

Fig. 3. Missing p_T distribution for $e^+e^- \to L^+L^- \to 4$ jets + 2 neutrinos at $E_b = 35$ GeV, $m_L = 0.9E_b$. The effect of a non-zero neutrino mass is shown: $m_{\nu_L} = 0$ (dashed line), $m_{\nu_L} = 0.3m_L$ (solid line), $m_{\nu_L} = 0.5m_L$ (dash-dotted line).

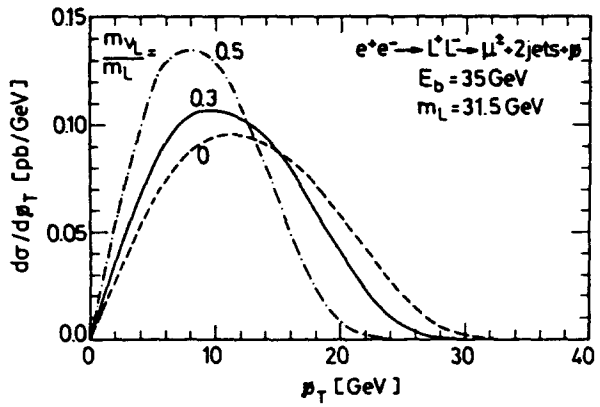

Fig. 4. $\not p_T$ distribution for $e^+e^- \to L^+L^- \to 2$ jets + $\mu^\pm$ + 3 neutrinos. E_b, m_L and m_{ν_L} are chosen as in fig. 3.

multijets will give a very clean signal for heavy lepton production within the standard model. In figs. 3 and 4 the resulting distributions of missing transverse momentum ($\not p_T$) are shown for a beam energy $E_b = 35$ GeV, a heavy lepton mass $m_L = 0.9E_b$ and three values of the ν_L mass: $m_{\nu_L} = 0, 0.3m_L, 0.5m_L$. Fig. 3 shows the $\not p_T$ distribution for 4 jet + $\not p_T$ events while fig. 4 is for 2 jets + $\mu^\pm$ + $\not p_T$ events: due to the additional muon neutrino the class (b) distribution (fig. 4) is somewhat harder than the one of the class (a) (fig. 3).

In figs. 5 to 7 the missing energy ($\not E$) signal is shown for 4 jets + $\not p$ events at three different energies: $E_b = 35$ GeV, 46.5 GeV = $\frac{1}{2}m_Z$, and 100 GeV respectively. Again we have chosen $m_L = 0.9E_b$ and the $m_{\nu_L} = 0, 0.1m_L, 0.3m_L, 0.5m_L$ curves are given. Obviously the $\not E$ distributions are much more sensitive to a non-zero neutrino mass than the $\not p_T$ signal: observation of $m_{\nu_L} \neq 0$ appears to be possible down to $m_{\nu_L} = 0.1m_L$ at $E_b < m_W$. While the $\not E$-distributions are very similar at $E_b = 35$ GeV and $E_b = \frac{1}{2}m_Z$ (this actually is true for all the distributions shown in figs. 3–10), a much higher sensitivity for $m_{\nu_L} \neq 0$ is obtained at $E_b = 100$ GeV, $m_L = 90$ GeV (fig. 7). This sensitivity is simply a consequence of the fact that a 90 GeV heavy lepton predominantly decays into a real W plus a ν_L if m_{ν_L} is small enough. At $m_{\nu_L} \approx 8$ GeV already, the threshold for the $L \to \nu_L W$ decay mode is crossed, resulting in a very strong m_{ν_L} dependence of differential cross sections. It should be noted that the $\not E$ distributions are more sensitive to the QED radiative corrections than the $\not p_T$ distributions due to the emission of collinear hard photons in the initial channel. Realistic confrontations of the $\not E$ distributions with experiments should include the radiative effects as well. Here we show qualitative trends in order to examine what could be achieved in actual experiments.

At LEP/SLC and TRISTAN energies, a high sensitivity for a non-zero neutrino mass is also found in the dijet energy and dijet invariant mass distributions for the

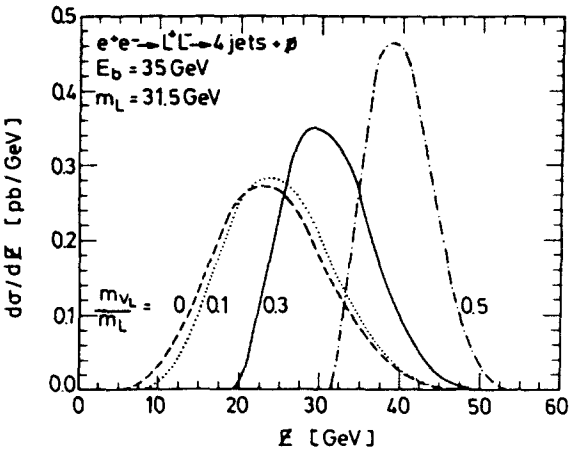

Fig. 5. Missing energy distribution for the 4 jets + 2 neutrinos decay mode of $L\bar{L}$ at $E_b = 35$ GeV, $m_L = 0.9E_b$. The curves are for $m_{\nu_L} = 0$ (dashed line), $m_{\nu_L} = 0.1m_L$ (dotted line), $m_{\nu_L} = 0.3m_L$ (solid line), and $m_{\nu_L} = 0.5m_L$ (dash-dotted line).

process $e^+e^- \to L^+L^- \to \mu^+ + 2$ jets + 3 neutrinos. In figs. 8 and 9 they are given for a machine operating at the Z mass assuming $m_L = 0.9E_b$. As mentioned earlier results for TRISTAN are very similar.

In fig. 10 the $\mu - e$ invariant mass distribution is given for the process $e^+e^- \to L\bar{L} \to e^+\mu^- + 4$ neutrinos at $E_b = 35$ GeV, $m_L = 0.9E_b$ and $m_{\nu_L} = (0, 0.1, 0.3, 0.5)m_L$. Sensitivity of this signal for neutrino mass measurements is not as high as in the dijet energy and dijet invariant mass distributions, and furthermore the $m_{\mu e}$

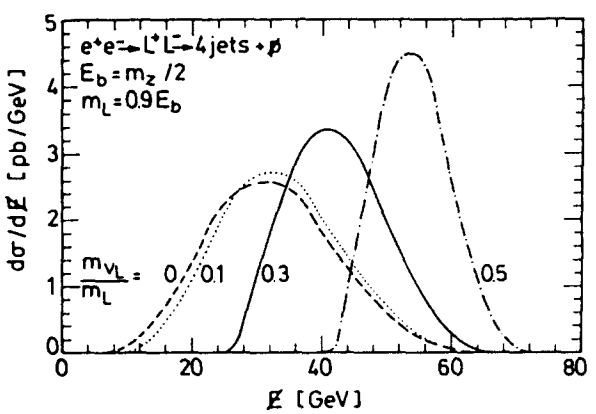

Fig. 6. Same as fig. 5 but for $E_b = \frac{1}{2}m_Z$.

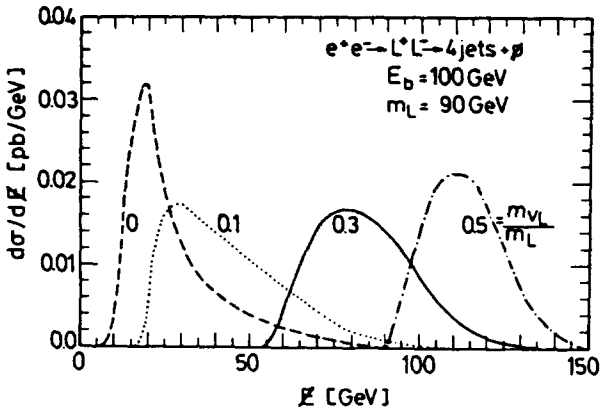

Fig. 7. Same as fig. 5 but for $E_b = 100$ GeV.

distribution will be affected in the lower mass region by the 28% contamination of secondary muons or electrons arising from the τ decay modes.

So far we have assumed the mass m_L of the heavy lepton to be known. The easiest and most precise way to measure it will probably be to follow the threshold behaviour of the ratio

$$R = \frac{\sigma(e^+e^- \to L\bar{L})}{\sigma(e^+e^- \to \mu^+\mu^-)}. \tag{5.1}$$

If $2m_L$ is between TRISTAN and SLC/LEP-I energies, a method for measuring m_L at fixed beam energy $E_b = \frac{1}{2}m_Z$ is advantageous. Due to the almost axial coupling of Z to standard charged leptons the ratio R is proportional to β^3 due to the P-wave

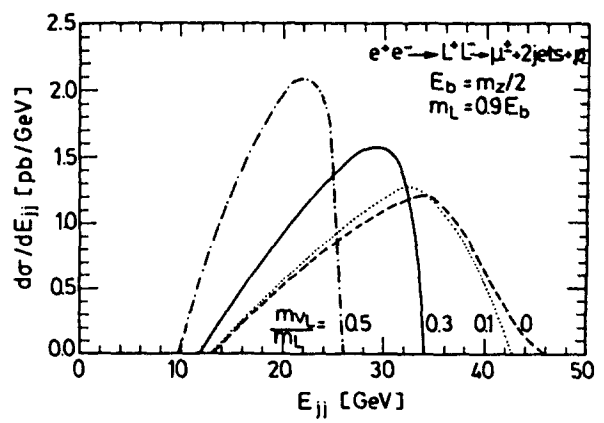

Fig. 8. $d\sigma/dE_{jj}$ for $e^+e^- \to L^+L^- \to \mu^+ + 2$ jets + 3 $(\bar{\nu})$'s at $E_b = \frac{1}{2}m_Z$, $m_L = 0.9E_b$. Choice of neutrino masses is as in fig. 5.

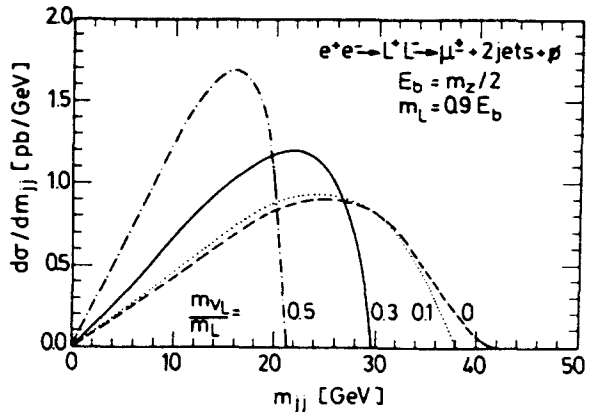

Fig. 9. Dijet invariant mass distribution for $E_b = \frac{1}{2}m_Z$, $m_L = 0.9E_b$, $m_{\nu L} = (0, 0.1, 0.3, 0.5)m_L$.

production, and measuring the $L\bar{L}$ production cross section allows a rather precise mass determination [4]. This method is of course very much dependent on the assumption of standard couplings of L to Z and W [4], and a complementary method is highly desirable. Here we suggest determining the dijet opening angle in the $L\bar{L} \to 2$ jets $+ \ell^{\pm} + \not{p}_T$ decay mode which measures the boost factor of the dijet system from the $(\bar{L})$ rest frame to the lab. frame. Figs. 11 and 12 show the resulting distributions for $m_L = 40, 41, 42$ GeV and $m_L = 29, 30$ GeV respectively. For both figures $E_b = \frac{1}{2}m_Z$ and $m_{\nu_L} = 0$ was chosen. Fig. 11 clearly reflects the strong β^3 threshold dependence, but at the same time the change in dijet angular distribution is apparent. This increase of dijet opening angle with increasing m_L is even more pronounced in fig. 12.

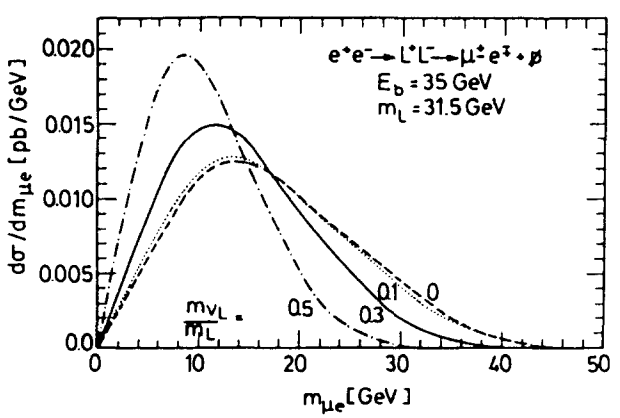

Fig. 10. $e^{\mp}\mu^{\pm}$ invariant mass distribution for the process $e^+e^- \to L^+L^- \to e^{\mp}\mu^{\pm} + 4$ neutrinos at $E_b = 35$ GeV, $m_L = 0.9E_b$. Neutrino masses are chosen as in fig. 5.

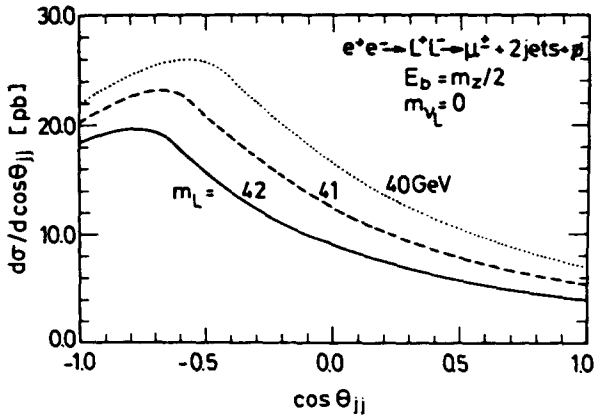

Fig. 11. Distribution of dijet opening angles for $E_b = \frac{1}{2}m_Z$, $m_{\nu_L} = 0$ and for $m_L = 42$ GeV (solid line), 41 GeV (dashed line), 40 GeV (dotted line).

The distributions shown so far are to a large extent given by kinematics, which seems to be sufficient to identify $L\bar{L}$ events, to measure neutrino masses etc. In order to get a handle on the dynamics and in particular on the V, A structure of the heavy lepton's couplings, angular distributions have to be analysed. The V, A-couplings of $L\bar{L}$ to Z determine the heavy lepton's polar angle distribution. As a tag on the direction of L, the direction of its decay muon or electron can be used. The resulting polar angle distribution of μ^- with respect to the e^- beam is shown in fig. 13 for standard model couplings, at $E_b = \frac{1}{2}m_Z$, $m_L = 0.9E_b$ and $m_{\nu_L} = 0$. It reproduces the angular distribution of its parent heavy lepton (the solid line in fig. 13) rather poorly, because $L\bar{L}$ production too close to the threshold is considered.

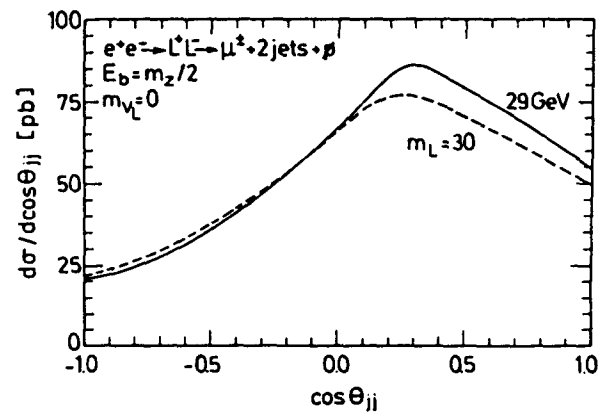

Fig. 12. Same as fig. 11 but for $m_L = 30$ GeV (dashed line) and $m_L = 29$ GeV (solid line).

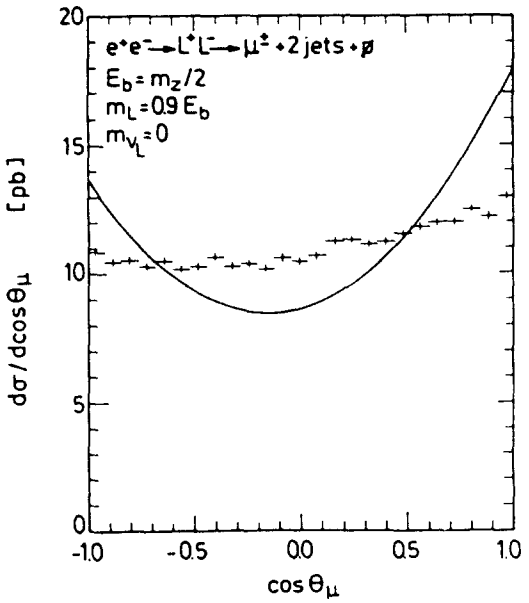

Fig. 13. Polar angle distribution of the decay muon in the process $e^+e^- \to L^+L^- \to \mu^+ + 2$ jets + 3 neutrinos at $E_b = \frac{1}{2}m_Z$ for $m_L = 0.9E_b$, $m_{\nu_L} = 0$. The symbols indicate the error of the Monte Carlo integration. The solid line shows the $\cos\theta$ distribution of the parent heavy lepton.

Nevertheless it should be possible to determine the heavy lepton forward-backward charge asymmetry this way.

Use of the total momentum of the dijet system recoiling against a μ^+ or e^+ allows for a much improved L polar angle distribution. Because in the decay $L \to \nu_L \bar{q}_2 q_3$ only the neutrino ν_L remains unobserved, kinematics allows us to determine the magnitude of the component of the neutrino momentum perpendicular to the dijet momentum, p_T, once an upper bound on m_{ν_L} has been set. Denoting the ν_L momentum by p_1 and the dijet momentum by $p_2 + p_3$ as in fig. 1 we indeed find

$$p_1 \cdot (p_2 + p_3) = (E_b - E_{jj}) E_{jj} + \tfrac{1}{2}\left(m_{jj}^2 + m_{\nu_L}^2 - m_L^2\right), \tag{5.2a}$$

$$p_1^2 = (E_b - E_{jj})^2 - m_{\nu_L}^2, \tag{5.2b}$$

and

$$|p_{1T}| = \left| p_1 - \frac{p_1 \cdot (p_2 + p_3)}{(p_2 + p_3)^2}(p_2 + p_3) \right|$$

$$= \left[p_1^2 - \frac{(p_1 \cdot (p_2 + p_3))^2}{E_{jj}^2 - m_{jj}^2} \right]^{1/2} \tag{5.3}$$

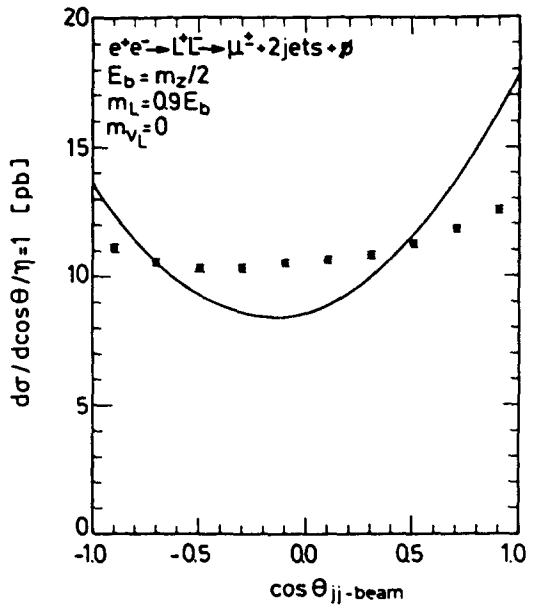

Fig. 14. Polar angle distribution of the dijet system in the process $e^+e^- \to L^+L^- \to \mu^+ + 2$ jets + 3 neutrinos. Parameters and symbols as in fig. 13.

can hence be determined experimentally for each event. Since the dijet direction is a good measure of the heavy lepton direction if $|p_{LT}|$ is small, a cut on

$$\eta = |p_{LT}|/E_b \tag{5.4}$$

will considerably improve the correlation between dijet and L angular distributions, as is clearly visible in figs. 14 and 15. The price to be paid for the $\eta \leqslant 0.2$ cut is a loss in statistics by roughly a factor of 3.

While the dijet angular distribution (with respect to the beam axis) is sensitive to the V, A structure of the production amplitude, the correlation of light lepton and dijet directions can distinguish between V + A and V − A coupling of the $(\nu_L L)$ doublet to $W^{\pm}$. This is because the L^- and μ^- momenta prefer to be aligned when both couple to left-handed weak currents, while the μ^- will rather go backwards to the L^- momentum, if the parent L^- has V + A coupling to W^-. The effect is clearly visible in fig. 16.

A μ or e going in a direction opposite to its parent, will on the average have a lower energy in the laboratory than a lepton arising from a left-handed L. Figs. 17 and 18 show the difference between V + A coupling and V − A coupling for the muon energy and the dilepton mass distributions. Distinguishing V + A from V − A appears to be straightforward and it also should be possible to determine the vector and axial couplings to the W individually.

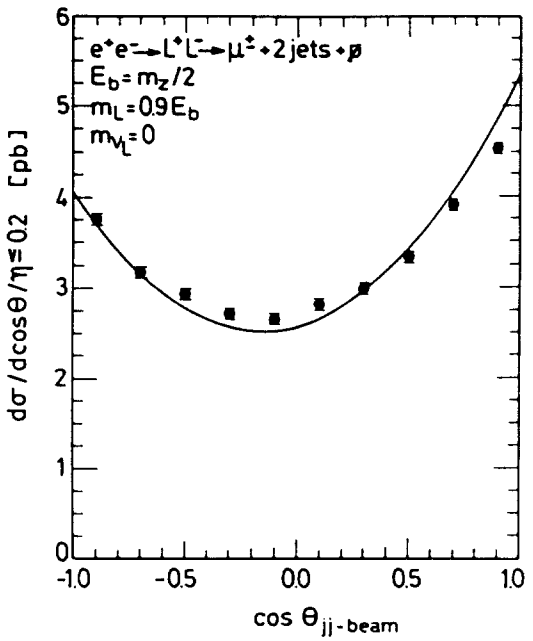

Fig. 15. Same as fig. 14 but for $\eta \leq 0.2$ (see text).

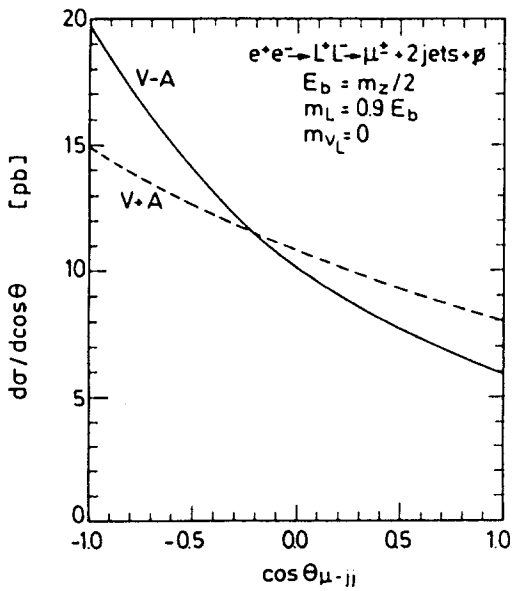

Fig. 16. Distribution of angles between muon and dijet system in $e^+e^- \to L^+L^- \to \mu^+ + 2$ jets + 3 neutrinos for V − A (solid line) and V + A (dashed line) coupling of $L\nu_L$ to W. $E_b = \frac{1}{2}m_Z$, $m_L = 0.9E_b$ and $m_{\nu_L} = 0$ were chosen.

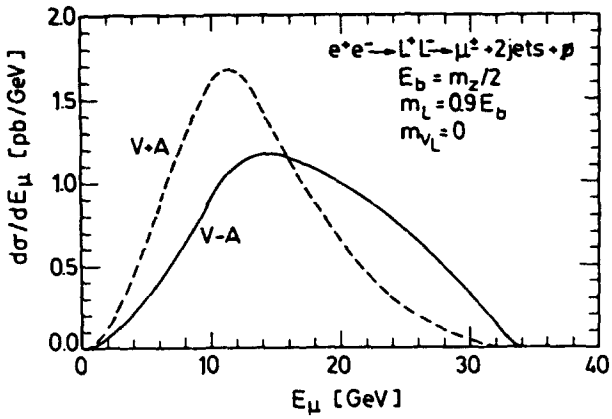

Fig. 17. Muon energy distribution for the lepton-dijet signal. The curves are given for an $m_L = 0.9E_b$ ($E_b = \frac{1}{2}m_Z$) heavy lepton with V + A (dashed line) and V − A (solid line) weak interactions. Again $m_{\nu_L} = 0$.

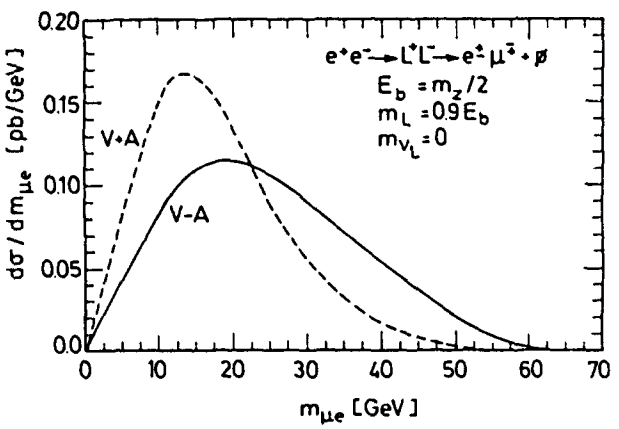

Fig. 18. Dilepton mass distribution for $e^+e^- \to L^+L^- \to e^\pm\mu^\mp$ + 4 neutrinos. Parameters and couplings as in fig. 17.

6. Heavy neutrino production

The expressions derived in sect. 4 for heavy charged lepton production and decay amplitudes can directly be used for massive neutrino (N) production and decay: it suffices to replace the heavy charged lepton couplings by the appropriate neutrino couplings. In particular $g_a^{\gamma NN} = 0$ in the production amplitude, and in the decay $N \to \ell^- +$(virtual) W^+ a mixing angle $U_{N\ell}$ has to be introduced. If N is a Majorana particle, N and $\overline{N}$ have to be treated as identical particles. The production

amplitude is then obtained from eq. (4.5) by choosing appropriate couplings and by antisymmetrizing it in (q_1, σ_1) and (q_2, σ_2).

Determining the properties of a heavy neutrino will actually be easier than for a charged heavy lepton. This is so because more of the final state fermions will carry charge, the dominant decay mode usually giving two charged leptons and four jets. If the N mass is sufficiently small and/or if the mixing angle $U_{\mathrm{N}\ell}$ is tiny it may even be possible to determine the N lifetime from its decay in flight.

If there exist large flavor changing neutral current couplings between neutrinos $g_a^{Z\mathrm{N}_1\mathrm{N}_2}$, as in some models with mirror fermions [19], then different mass neutrinos can be pair produced and their decays can proceed via both charged and neutral current. Our general formula with arbitrary mass and couplings will be most suited to study the consequences of such models.

7. Polarized beams

It is clear that longitudinal polarization of the colliding e^+e^- beams will be very useful for a detailed study of electroweak theory. Transverse polarization of the beams is not only necessary to establish the longitudinal polarization but it can, in itself, be useful for probing non-standard (scalar [20] or magnetic [21]) couplings of electrons. In practice, the beam polarization will be only partially longitudinal and partially transverse.

The helicity amplitudes given in sect. 4 can be used directly to produce cross-sections for longitudinally polarized beams. For arbitrary polarization direction we follow the notation used by Olsen et al. [22]. We describe a general state of partial or complete polarization of the e^+ and e^- beams by the polarization vectors

$$s_\pm^\mu = P_\pm^{\mathrm{T}}(0, \hat{s}_\pm) + P_\pm^{\mathrm{L}}(|\boldsymbol{p}_\pm|, E_\pm \hat{\boldsymbol{p}}_\pm)/m, \tag{7.1}$$

where $\hat{s}_\pm$ are unit 3-vectors perpendicular to the beam directions $\hat{\boldsymbol{p}}_+$ and $\hat{\boldsymbol{p}}_-$. $P_\pm^{\mathrm{T}}$ denote the degrees of transverse polarization and $P_\pm^{\mathrm{L}}$ the degrees of longitudinal polarization and they are bounded by

$$\rho_\pm = \left[\left(P_\pm^{\mathrm{T}}\right)^2 + \left(P_\pm^{\mathrm{L}}\right)^2\right]^{1/2} \leqslant 1. \tag{7.2}$$

We introduce

$$\cos\zeta_\pm = P_\pm^{\mathrm{L}}/\rho_\pm, \qquad \sin\zeta_\pm = P_\pm^{\mathrm{T}}/\rho_\pm \tag{7.3}$$

in order to obtain the unit space-like 4-vectors

$$n_\pm^\mu = \sin\zeta_\pm(0, \hat{s}_\pm) + \cos\zeta_\pm(|\boldsymbol{p}_\pm|, E_\pm \hat{\boldsymbol{p}}_\pm)/m, \tag{7.4}$$

which define the projectors onto spinors describing electrons and positrons polarized

in the $\varepsilon_\pm n_\pm$ ($\varepsilon_\pm = +$ or $-$) direction:

$$u(p_-, \varepsilon_- n_-) = \tfrac{1}{2}(1 + \varepsilon_- \gamma_5 \not{n}_-) u(p_-, \varepsilon_- n_-). \tag{7.5a}$$

$$v(p_+, \varepsilon_+ n_+) = \tfrac{1}{2}(1 + \varepsilon_+ \gamma_5 \not{n}_+) v(p_+, \varepsilon_+ n_+). \tag{7.5b}$$

It is straightforward to expand these spinors in terms of helicity eigenstates

$$u(p_-, \lambda) = \begin{pmatrix} u_-(p_-, \lambda) \\ u_+(p_-, \lambda) \end{pmatrix}. \tag{7.6a}$$

$$v(p_+, \lambda) = \begin{pmatrix} v_-(p_+, \lambda) \\ v_+(p_+, \lambda) \end{pmatrix}. \tag{7.6b}$$

defined in eq. (3.20). In the massless limit ($m \to 0$) we find

$$\begin{pmatrix} u(p_-, n_-) \\ u(p_-, -n_-) \end{pmatrix} = \sum_\lambda U_{\cdot,\lambda} u(p_-, \lambda) = \begin{pmatrix} \cos\tfrac{1}{2}\zeta_- & \sin\tfrac{1}{2}\zeta_- \, e^{i\alpha} \\ -\sin\tfrac{1}{2}\zeta_- \, e^{-i\alpha} & \cos\tfrac{1}{2}\zeta_- \end{pmatrix} \begin{pmatrix} u(p_-, +) \\ u(p_-, -) \end{pmatrix} \tag{7.7a}$$

$$\begin{pmatrix} v(p_+, n_+) \\ v(p_+, -n_+) \end{pmatrix} = \sum_\lambda V_{\cdot,\lambda} v(p_+, \lambda) = \begin{pmatrix} \cos\tfrac{1}{2}\zeta_+ & \sin\tfrac{1}{2}\zeta_+ \, e^{i\alpha_+} \\ -\sin\tfrac{1}{2}\zeta_+ \, e^{-i\alpha_+} & \cos\tfrac{1}{2}\zeta_+ \end{pmatrix} \begin{pmatrix} v(p_+, +) \\ v(p_+, -) \end{pmatrix}. \tag{7.7b}$$

The phase factors $\exp(i\alpha_\pm)$ are given by the orientation of $\hat{\boldsymbol{p}}_\pm$ and $\hat{\boldsymbol{s}}_\pm$ in the coordinate frame. To be specific we choose

$$\hat{\boldsymbol{p}}_\pm = (\sin\theta_\pm \cos\phi_\pm, \sin\theta_\pm \sin\phi_\pm, \cos\theta_\pm), \tag{7.8}$$

$$\hat{\boldsymbol{s}}_\pm = \begin{pmatrix} \sin\psi_\pm \sin\phi_\pm + \cos\psi_\pm \cos\theta_\pm \cos\phi_\pm, \\ -\sin\psi_\pm \cos\phi_\pm + \cos\psi_\pm \cos\theta_\pm \sin\phi_\pm, \\ -\sin\theta_\pm \cos\psi_\pm \end{pmatrix}^{\mathrm{T}}, \tag{7.9}$$

then we find

$$\alpha_\pm = \phi_\pm - \psi_\pm. \tag{7.10}$$

We can now relate arbitrary polarization amplitudes to helicity amplitudes. For an arbitrary process $e^+e^- \to X$ we use $\mathcal{M}_{\cdot,\cdot}$ to denote the amplitude for an electron polarized in the $\varepsilon_- n_-$ and a positron polarized in the $\varepsilon_+ n_+$ direction and

$\mathcal{M}(\kappa_1, \kappa_2)$ for the corresponding helicity amplitude (treatment of final state polarizations is implicit in the sequel). From eq. (7.7) we find

$$\mathcal{M}_{\sigma_1 \sigma_2} = \sum_{\kappa_1, \kappa_2} U_{\sigma_1 \kappa_1} \mathcal{M}(\kappa_1, \kappa_2) V^{\dagger}_{\kappa_2 \sigma_2} . \tag{7.11}$$

The polarization vector $s_\pm$ in eq. (7.1) describes $e^\pm$ beams polarized with probability $\frac{1}{2}(1 + \rho_\pm)$ in $n_\pm$ direction and probability $\frac{1}{2}(1 - \rho_\pm)$ in $-n_\pm$ direction. The polarization weighted squared matrix element is therefore

$$\begin{aligned} \overline{\sum_{\text{pol}}} |\mathcal{M}|^2 &\equiv \sum_{\sigma_1, \sigma_2 = \pm} \tfrac{1}{2}(1 + \varepsilon_+ \rho_+) \tfrac{1}{2}(1 + \varepsilon_- \rho_-) |\mathcal{M}_{\sigma_1 \sigma_2}|^2 \\ &= \sum_{\kappa_1 \kappa_2 \kappa_1' \kappa_2'} \mathcal{M}(\kappa_1, \kappa_2) P^+_{\kappa_2 \kappa_2'} \mathcal{M}^*(\kappa_1', \kappa_2') P_{\kappa_1' \kappa_1} , \end{aligned} \tag{7.12}$$

and the polarization matrices $P^\pm$ are given by

$$P_{\kappa_1' \kappa_1} = \sum_{\sigma = \pm} U^{\dagger}_{\kappa_1' \sigma} \tfrac{1}{2}(1 + \varepsilon_- \rho_-) U_{\sigma \kappa_1} = \tfrac{1}{2} \begin{pmatrix} 1 + P^{\mathrm{L}}_- & P^{\mathrm{T}}_- e^{i\alpha_-} \\ P^{\mathrm{T}}_- e^{-i\alpha_-} & 1 - P^{\mathrm{L}}_- \end{pmatrix}, \tag{7.13a}$$

$$P^+_{\kappa_2 \kappa_2'} = \sum_{\sigma = \pm} V^{\dagger}_{\kappa_2' \sigma} \tfrac{1}{2}(1 + \varepsilon_+ \rho_+) V_{\sigma \kappa_2} = \tfrac{1}{2} \begin{pmatrix} 1 + P^{\mathrm{L}}_+ & P^{\mathrm{T}}_+ e^{i\alpha_+} \\ P^{\mathrm{T}}_+ e^{-i\alpha_+} & 1 - P^{\mathrm{L}}_+ \end{pmatrix}. \tag{7.13b}$$

In many applications, and in particular for $\mathrm{L}\bar{\mathrm{L}}$ production, the relation

$$\mathcal{M}(\kappa_1, \kappa_2) = \delta_{\kappa_1, \kappa_2} \mathcal{M}(\kappa_1, -\kappa_1) \tag{7.14}$$

holds, when the electron mass is neglected. In this case eq. (7.12) can be simplified further to read

$$\overline{\sum_{\text{pol}}} |\mathcal{M}|^2 = \sum_{\kappa_1, \kappa_1'} \mathcal{M}^*(\kappa_1', -\kappa_1') P^+_{\kappa_1' \kappa_1} \mathcal{M}(\kappa_1, -\kappa_1), \tag{7.15}$$

with

$$P^{+\,-}_{\kappa_1' \kappa_1} = \tfrac{1}{4} \begin{pmatrix} (1 + P^{\mathrm{L}}_-)(1 - P^{\mathrm{L}}_+) & P^{\mathrm{T}}_- P^{\mathrm{T}}_+ e^{i(\alpha_- - \alpha_+)} \\ P^{\mathrm{T}}_- P^{\mathrm{T}}_+ e^{-i(\alpha_- - \alpha_+)} & (1 - P^{\mathrm{L}}_-)(1 + P^{\mathrm{L}}_+) \end{pmatrix}, \tag{7.16}$$

which, together with the helicity amplitudes presented in sect. 4, allows to study $\mathrm{L}\bar{\mathrm{L}}$ production for arbitrary beam polarizations. For the special case $\hat{p}_\pm = (0, 0, \mp 1)$ and $\hat{s}_\pm = (0, \pm 1, 0)$ (where the colliding beams run along the z-axis and the transverse polarizations are along the y-axis), one obtains $\alpha_\pm = \pm \frac{1}{2}\pi$ in eq. (7.10) and accordingly the two phase factors of eq. (7.16) are both -1.

8. Conclusions

We presented helicity amplitudes for heavy lepton pair production (including their three-body decays) in e^+e^- collisions with arbitrary vector/axial vector couplings and with arbitrary final fermion masses. The amplitudes are cast into a form which makes their direct numerical evaluation efficient. By studying four-jet, dijet plus single lepton, and dilepton signals, we exemplified the measurement of the couplings, of the associated neutrino mass, and of the heavy lepton mass itself near the threshold at TRISTAN, SLC/LEP-I, and LEP-II energies. We commented on the use of our amplitudes for studying heavy neutrino pair production signals and for studying polarized beam effects.

For completeness we presented in sect. 3 a self-contained description of our method to evaluate arbitrary tree amplitudes with external fermions and vector bosons. The method requires minimal algebraic manipulation in the Weyl spinor basis which leads to a unique standard expression of the amplitude, whose form allows its efficient numerical evaluation. It gives a general prescription; no clever choice of polarization vectors, no trick for gamma matrix contractions nor special treatment for massive fermions are required. One of the key features of our method is that we express the wave function of a fermion or a vector boson in a given polarization state in terms of only its own momentum in an arbitrary Lorentz frame. Because of this the full polarization amplitudes are expressed in an arbitrary frame and the Lorentz invariance of the polarization summed squared amplitude provides us with a very non-trivial check of the overall calculation.

The authors wish to thank K.-L. Au, H. Baer, N. Brown, J. Cortés, K. Hikasa, G. Ingelman, S. Komamiya, A.D. Martin and X. Tata for valuable discussions. One of the authors (K.H.) would like to express his gratitude to A.D. Martin for kind hospitality at the University of Durham. This research was supported in part by the Science and Engineering Research Council of Great Britain.

References

[1] UA1 Collaboration, G. Arnison et al., Phys. Lett. 147B (1984) 493
[2] V. Barger, H. Baer, K. Hagiwara and R.J.N. Phillips, Phys. Rev. D30 (1984) 947;
H. Baer, talk at the New Particle '85 Conference, Madison (May 8–11, 1985)
[3] D. Cline and C. Rubbia, Phys. Lett. 127B (1983) 277;
V. Barger, H. Baer, A.D. Martin, E.W.N. Glover and R.J.N. Phillips, Phys. Lett. 133B (1983) 449;
Phys. Rev. D29 (1984) 2020
[4] H. Baer, V. Barger and R.J.N. Phillips, Phys. Rev. D32 (1985) 688
[5] M.L. Perl, Ann. Rev. Nucl. Part. Sci. 30 (1980) 299;
L.B. Okun, Leptons and quarks (North-Holland, Amsterdam, 1982)
[6] Y.S. Tsai, Phys Rev. D4 (1971) 2821;
S.Y. Pi and A.I. Sanda, Ann. of Phys. 106 (1977) 134; 106 (1977) 171
[7] H. Kühn and F. Wagner, Nucl. Phys. B236 (1984) 16
[8] J.D. Bjorken and M.C. Chew, Phys. Rev. D6 (1972) 471

[9] K.J.F. Gaemers and G.J. Gounaris, Z. Phys. C1 (1979) 259;
M. Hellmund and G. Ranft, Z. Phys. C12 (1982) 333;
J. Cortés, K. Hagiwara and F. Herzog, Phys. Rev. D28 (1983) 2311
[10] G. Farrar and F. Neri, Phys. Lett. 130B (1983) 109;
J. Cortés, unpublished (1983);
G. Passarino, Nucl. Phys. B237 (1984) 249;
B.K. Sawhill, SLAC report PUB-3564 (1985);
A. Kersch and F. Scheck, Nucl. Phys. B263 (1986) 475
[11] CALKUL Collaboration, Phys. Lett. 105B (1981) 215; 114B (1982) 203; Nucl. Phys. B206 (1982) 53; B206 (1982) 61; B239 (1984) 382; B239 (1984) 395
[12] R. Kleiss, Nucl. Phys. B241 (1984) 61
[13] F.A. Berends, P.H. Daverveldt and R. Kleiss, Nucl. Phys. B253 (1985) 411;
R. Kleiss and W.J. Stirling, Nucl. Phys. B262 (1985) 235
[14] F. Herzog and Z. Kunszt, Phys. Lett. 157B (1985) 430;
M. Golden and S. Sharpe, Nucl. Phys. B261 (1985) 217
[15] J.D. Bjorken and S.D. Drell, Relativistic quantum mechanics, and Relativistic quantum fields (McGraw-Hill, New York, 1964)
[16] J. Wess and J. Bagger, Supersymmetry and supergravity (Princeton Univ. Press, Princeton, 1983)
[17] G.P. Lepage, Cornell University preprint CLNS-80/447 (1980); J. Comp. Phys. 27 (1978) 192
[18] P. Aurenche and R. Kinnunen, Z. Phys. C28 (1985) 261;
R. Odorico, University of Bologna preprint IFUB 85/1 (1985);
E.W.N. Glover and A.D. Martin, Z. Phys. C, to be published
[19] J. Bagger and S. Dimopoulos, Nucl. Phys. B244 (1984) 247
[20] K. Hikasa, Phys. Lett. 143B (1984) 266;
S. Narison and J.C. Wallet, Phys. Lett. 158B (1985) 355
[21] K. Hikasa, private communication
[22] H.A. Olsen, P. Osland and I. Øverbo, Nucl. Phys. B171 (1980) 209;
T. Sjöstrand, Comput. Phys. Comm. 28 (1983) 229